



1

Ba incorporation in benthic foraminifera

2

3 Lennart J de Nooijer^{1*}, Anieke Brombacher^{2,a}, Antje Mewes³, Gerald Langer⁴, Gernot Nehrke³,

4 Jelle Bijma³, Gert-Jan Reichart^{1,2}

5

6 ¹Royal Netherlands Institute of Sea Research, Dept of Geology and Chemical Oceanography,

7 Landsdiep 4, 1797 SZ 't Horntje, The Netherlands

8 *Corresponding author: ldenooijer@nioz.nl

9 ²Utrecht University, Faculty of Geosciences, Budapestlaan 4, 3584 CD Utrecht, The

10 Netherlands

11 ³Alfred-Wegener-Institut Helmholtz-Zentrum für Polar- und Meeresforschung, Biogeosciences

12 section, Am Handelshafen 12, 27570 Bremerhaven, Germany

13 ⁴The Marine Biological Association of the United Kingdom, The Laboratory, Citadel Hill,

14 Plymouth, Devon, PL1 2PB, UK

15 ^anow at: National Oceanography Centre, University of Southampton, Waterfront Campus,

16 European Way, Southampton SO14 3ZH, UK

17

18 Abstract

19 Barium (Ba) incorporated in the calcite of many foraminiferal species is proportional to the

20 concentration of Ba in seawater. Since the open ocean concentration of Ba closely follows

21 seawater alkalinity, foraminiferal Ba/Ca can be used to reconstruct the latter. Alternatively,

22 Ba/Ca from foraminiferal shells can also be used to reconstruct salinity in coastal settings where

23 seawater Ba concentration corresponds to salinity as rivers contain much more Ba than

24 seawater. Incorporation of a number of minor and trace elements is known to vary (greatly)

25 between foraminiferal species and application of element/Ca ratios thus requires the use of



26 species-specific calibrations. Here we show that calcite Ba/Ca correlates positively and linearly
27 with seawater Ba/Ca in cultured specimens of two species of benthic foraminifera,
28 *Heterostegina depressa* and *Amphistegina lessonii*. The slopes of the regression, however, vary
29 2-3 fold between these two species (0.33 and 0.78, respectively). This difference in Ba-
30 partitioning resembles the difference in partitioning of other elements (Mg, Sr, B, Li and Na)
31 in these foraminiferal taxa. A general trend across element partitioning for different species is
32 described, which may help developing new applications of trace elements in foraminiferal
33 calcite in reconstructing past seawater chemistry.

34

35 Keywords: foraminifera, Ba/Ca, proxies

36

37 **1 Introduction**

38 Incorporation of barium (Ba) in foraminiferal calcite is proportional to seawater barium
39 concentrations (e.g. Lea and Boyle, 1989; 1990; Lea and Spero, 1994). Since open ocean and
40 coastal seawater Ba concentrations correlate well to total alkalinity and salinity, respectively,
41 Ba/Ca of fossil foraminiferal calcite has been used to reconstruct these two parameters (e.g.
42 Lea, 1995; Weldeab et al., 2007; 2014; Bahr et al., 2013). Application of Ba/Ca for such
43 reconstructions, however, critically depends on the prerequisite that temperature and salinity
44 (Lea and Spero, 1994; Hönisch et al., 2011) and photosymbiont activity (Lea and Spero, 1992;
45 Hönisch et al., 2011) do not affect Ba/Ca of planktonic foraminifera. Still, Ba/Ca ratios are
46 known to vary within chamber walls of crust-producing planktonic foraminifera (Eggins et al.,
47 2003; Hathorne et al., 2009). Like Mg/Ca, the values for Ba in crust carbonate are lower, which
48 cannot be (solely) explained by migration to greater water depths during crust formation
49 (Hathorne et al., 2009). This argues for an unknown additional imprint on Ba incorporation. On
50 an intra-test scale, the distributions of Mg and Ba within the test wall of *Pulleniatina*



51 *obliquiloculata* have been shown to co-vary to some extent, with maximum concentrations
52 often, but not always, coinciding with the ‘organic linings’ (Kunioka et al., 2006). For some
53 other elements, including Mg and Sr, incorporation has been shown to be inter-dependent (e.g.
54 Mewes et al., 2015). This interdependency varies between pairs of elements and is explained
55 by a combination of simultaneous fractionation by the same process (e.g. Langer et al., 2016)
56 and by involvement of different processes during calcification (Nehrke et al., 2013). These
57 models and experimental results may imply that also the incorporation of Ba could be
58 influenced by these physiological processes and/ or the same fractionation process during
59 calcite precipitation (e.g. through lattice distortion; Mucci and Morse, 1983; Mewes et al.,
60 2015).

61 So far, Ba/Ca values have been reported for planktonic (Boyle, 1981; Lea and
62 Boyle, 1991; Lea and Spero, 1992; 1994; Hönisch et al., 2011; Marr et al., 2013; Hoffmann et
63 al., 2014) and low-Mg benthic species (Lea, 1995; Lea and Boyle, 1989; 1990; 1993; Reichart
64 et al., 2003). Although Mg/Ca is known to vary greatly between (benthic) foraminiferal species
65 (between ~1 and ~150 mmol/mol; Toyofuku et al., 2000; Bentov and Erez, 2006; Wit et al.,
66 2012) it remains to be investigated whether Ba/Ca also varies between benthic species with
67 different Mg/Ca. Ba/Ca in the planktonic species may be used to reconstruct (changes in) open
68 ocean alkalinity (Lea, 1995) and those published for benthics are more suitable to reconstruct
69 salinity in coastal and shelf seas (Weldeab et al., 2007; 2014; Bahr et al., 2013). The range in
70 Mg/Ca is known particularly for benthic foraminifera (e.g. Toyofuku et al., 2011; Sadekov et
71 al., 2014) and inter-species variability in Ba incorporation may therefore particularly hamper
72 application of (benthic) foraminiferal Ba/Ca. Here we present results from culture studies using
73 the larger benthic foraminifera, *Amphistegina lessonii* and *Heterostegina depressa*, two species
74 with different Mg/Ca (~50 mmol/mol; Segev and Erez, 2006 and ~120 mmol/mol; Dueñas-
75 Bohórquez et al., 2011, respectively). These results are compared to Ba/Ca in these species



76 from field samples. Together, calibration of Ba/Ca in these species against seawater Ba/Ca
77 allows evaluation and application of incorporated Ba across a wider range of foraminiferal taxa,
78 with contrasting element composition of their shell.

79

80 2 Methods

81 2.1 Culture media

82 To determine Ba/Ca partitioning, benthic foraminiferal culture experiments were set up with
83 five different seawater Ba/Ca ratios (54-92 $\mu\text{mol/mol}$). Media were prepared by increasing
84 $[\text{Ba}^{2+}]_{\text{sw}}$ while keeping the $[\text{Ca}^{2+}]_{\text{sw}}$ constant. The range of $[\text{Ba}^{2+}]$ used in these experiments
85 exceeds the range of concentrations found naturally and allows testing the applicability of
86 partition coefficients under conditions with artificially high seawater Ba/Ca. Seawater is only
87 slightly undersaturated with respect to barite (BaSO_4) and an increase in $[\text{Ba}^{2+}]$ in the sea water
88 will cause barite precipitation (Langer et al., 2009). To be able to increase $[\text{Ba}^{2+}]$ beyond its
89 natural range, artificial seawater was prepared with lower sulphate contents. All other salts were
90 added according to the recipe of Kester et al. (1967). As *Amphistegina lessonii* and
91 *Heterostegina depressa* do not grow well in 100% artificial seawater, the prepared media were
92 mixed with natural seawater in a ratio 9:1 (Mewes et al., 2014). To double check concentrations
93 and determine potential loss of elements due to precipitation, sorption and/or scavenging,
94 element concentrations of the culture media were determined by ICP-OES at the Alfred-
95 Wegener-Institute in Bremerhaven, except for Ba which was measured by ICP-MS at Utrecht
96 University (Table 1).

97 Culture media pH was adjusted to 8.0 by adding NaOH (1 M) to the prepared media. Before
98 the start of the experiments, dissolved inorganic carbon (DIC) and total alkalinity were
99 measured at the Alfred-Wegener-Institute. DIC was measured photometrically in triplicates
100 with a TRAACS CS800 QuAAtro autoanalyser with an average reproducibility of $\pm 10 \mu\text{mol}$



101 L⁻¹. Alkalinity was calculated from linear Gran plots (Gran, 1952) after triplicate potentiometric
102 titration (Bradshaw et al., 1981) using a TitroLine alpha plus auto sampler (Schott
103 Instruments). Parameters of the total carbonate system were calculated from temperature,
104 salinity, DIC and alkalinity using the program CO2SYS (Lewis and Wallace, 1998) adapted to
105 Excel by (Pierrot et al., 2006). The equilibrium constants K1 and K2 from Mehrbach et al.
106 (1973), as reformulated by Dickson and Millero (1987) were used (Table 1).

107

108 2.2 Foraminiferal culturing

109 Living specimens of *A. lessonii* and *H. depressa* were isolated from sediment collected at the
110 tropical aquarium of Burger's Zoo (Arnhem, The Netherlands) in August 2012 and transferred
111 to the Alfred-Wegener-Institute for the culture experiments. Healthy individuals of *A. lessonii*
112 showing pseudopodial activity, a dark brown cytoplasm and minimal signs of bleaching were
113 handpicked with a small brush under a Zeiss Stereo microscope and transferred to well plates.
114 Adult specimens of *H. depressa* were picked directly from the aquarium with soft tweezers.
115 After two weeks several individuals of both species underwent asexual reproduction. Individual
116 *H. depressa* parent cells produced sufficient numbers of juveniles to study separate clone
117 groups. Approximately 20 juveniles with two or three chambers from the same parent were
118 selected for every treatment and divided over two Petri dishes (diameter 55 mm). In total, two
119 clone groups were used in the experiments resulting in a total of at least 40 individuals per
120 treatment. Specimens of *A. lessonii* did not produce sufficient numbers of juveniles for analysis
121 of separate clone groups. Therefore, approximately 60 juveniles with two or three chambers
122 from different parents were selected per treatment and distributed evenly over three Petri dishes.
123 All experiments were carried out in an adjustable incubator (RUMED Rubarth Aparate GmbH)
124 at a constant temperature of 25 °C. As both species are symbiont-bearing, a 12:12 light:dark
125 cycle was applied with a constant photon flux density of approximately 250 μmol photons m⁻²



126 $2s^{-1}$ during light hours. Pictures were taken weekly under a Zeiss Axiovert 200M inverted
127 microscope and maximal diameters of the shells were measured with the AxioVision software
128 to allow determining the chamber addition rates of the foraminifera in the experiments. The
129 experiments were terminated after six weeks.

130 All specimens were fed *Dunaliella salina* algae every three to four days. Although *A. lessonii*
131 hosts symbionts, this foraminiferal species does not exclusively rely on nutrients from their
132 symbionts, but also ingests algae (Lee, 2006). To avoid changes in the barium concentration of
133 the culture media, foraminifera were diluted as little as possible by the solution containing the
134 food for the foraminifera. For this purpose, foraminifera were fed 50 μ l of a solution containing
135 algae that was centrifuged at 2000 rpm for 10 minutes. Algae concentrated at the bottom of the
136 tube were transferred to an empty tube with a pipette. To prevent changes in the culture media's
137 carbonate chemistry by algal photosynthesis the algae were killed by heating the concentrated
138 solution in an oven at 90 °C for 10 minutes. The cultures were transferred to new Petri dishes
139 every week to avoid excessive bacterial growth, potential build-up of waste products and
140 shortage of ions or nutrients. To prevent changes in salinity by evaporation media were
141 refreshed three days after the cultures were transferred to new dishes by pipetting approximately
142 5 ml of the old media out of the Petri dish and replacing it with the same volume of media from
143 the prepared batch.

144

145 2.3 Sample preparation and analysis

146 At the end of the culture experiment, specimens were cleaned by placing them in a 7% NaOCl
147 solution for approximately 30 minutes until completely bleached and organic material was
148 removed from the tests. This cleaning method is shown to have a similar impact on average
149 foraminiferal Ba/Ca values as cleaning with H₂O₂ (Pak et al., 2004). Specimens were then
150 rinsed three times for approximately 60 seconds in de-ionized water to remove the NaOCl and



151 any residual salts from the culture solutions. Cleaned foraminifera were put in an oven at 42 °C
152 until completely dry and mounted on sample holders using double sided adhesive tape.
153 Element composition of the calcite was determined using Laser Ablation-Inductively Coupled
154 Plasma-Mass Spectrometry (LA-ICP-MS) at Utrecht University (Reichert et al., 2003).
155 Monitored masses included ^{23}Na , ^{24}Mg , ^{26}Mg , ^{27}Al , ^{43}Ca , ^{44}Ca , ^{55}Mn , ^{88}Sr , ^{138}Ba and ^{238}U and
156 calibration was performed using a glass standard (NIST 610) that was ablated three times after
157 every 10-12 foraminiferal samples. Diameter of the ablation crater was set to 80 μm for all
158 specimens and pulse repetition rate was 6 Hz. The ablated calcite was measured and integrated
159 with respect to time. Energy density for the glass was higher than for the foraminifera (5 J/cm²
160 and 1 J/cm², respectively). Although the resulting difference in ablation characteristics is not
161 likely to affect obtained foraminiferal element concentrations (Hathorne et al., 2008),
162 foraminiferal element concentrations were compared to those from an in-house made calcite
163 standard with known element concentrations and ablated at the same energy density as the
164 foraminifera (Dueñas-Bohórquez et al., 2009). Due to the lamellar nature of Rotallid
165 foraminifera, the final chamber was generally too thin for reliable determination of element/Ca
166 ratios. Therefore, the F-1 chamber of *A. lessonii* was ablated for every specimen. For *H.*
167 *depressa*, walls of the final two chambers were commonly too thin for reliable chemical results
168 and, therefore, the F-2 chamber was analysed. For each species, the final 6-7 chambers of ten
169 sufficiently large specimens were ablated to analyse intra-specimen variability in Ba/Ca and to
170 detect potential ontogenetic trends in Ba incorporation.

171

172 Elemental concentrations were calculated from the ablation profiles with the Glitter software,
173 using ^{43}Ca as internal standard and values from Jochum et al. (2011) for concentrations of
174 elements in the NIST 610. This program integrates the ablation signal after subtracting the
175 background signal to calculate the elemental concentrations. To avoid contaminated intervals



176 of the ablation profile, sections with high ^{27}Al and ^{55}Mn counts were excluded from the analysis.
177 Ablation profiles with a duration shorter than 5 seconds were rejected as such short profiles are
178 unreliable due to poor counting statistics. Nine out of 188 ablation profiles were rejected for *A.*
179 *lessonii* and 7 out of 140 profiles from *H. depressa* were discarded, which is less than 5%.

180

181 *2.4 Field samples*

182 To compare the results from cultured specimens with Ba/Ca from specimens derived from
183 ‘naturel conditions’, a number of living specimens of both *A. lessonii* and *H. depressa* were
184 isolated from the Zoo’s stock and cleaned and prepared for LA-ICP-MS analyses as described
185 in 2.3. From both species, 7 specimens were ablated twice at the royal NIOZ using a
186 NWR193UC (New Wave Research) laser, containing an ArF Excimer laser (Existar) with deep
187 UV 193 nm wavelength and <4 ns pulse duration. Provided that the same reference material is
188 used, the use of multiple laser systems (see above) is shown not to bias obtained foraminiferal
189 element/Ca ratios (De Nooijer et al., 2014a). Laser ablation was performed with an energy
190 density of 1 J/cm² at a repetition rate of 6 Hz for calcite samples and an energy density of 5
191 J/cm² for the glass (NIST) standards. Helium was used as a carrier gas with a flow rate of 0.8
192 L/min for cell gas and 0.3 L/min for cup gas. From the laser chamber to the quadrupole ICP-
193 MS (iCAP-Q, Thermo Scientific), the He flow was mixed with ~0.4 L/min nebulizer Ar. Before
194 measuring the samples, the nebulizer gas, extraction lens, CCT focus lens and torch position
195 were automatically tuned for the highest sensitivity of ^{25}Mg by laser ablating MACS-3. The
196 masses measured by the ICP-MS were ^{23}Na , ^{24}Mg , ^{25}Mg , ^{27}Al , ^{43}Ca , ^{44}Ca , ^{88}Sr and ^{138}Ba . JCP-
197 1, MACS-3 and an in-house (foraminiferal) calcite standard (NFHS) were used for quality
198 control and measured every 10 foraminiferal samples. Internal reproducibility of the analyses
199 was all better than 9%, based on the three different carbonate standards used. Intensity data
200 were integrated, background subtracted, standardized internally to ^{43}Ca and calibrated against



201 the MACS-3 signal using a costume-built MATLAB routine within the program SILLS
202 (Guillong et al., 2008). Since ablation of the NIST SRM 610 and NIST SRM 612 could increase
203 the sodium background, they were only ablated and analyzed at the end of every sequence and
204 cones were cleaned before the next sequence. Accuracy of the analyses was better than 3%,
205 based on comparing the carbonate standards with internationally reported values (Okai et al.,
206 2002, Wilson et al., 2008). Signals were screened for surface contamination and parts of the
207 outside or inside of the shell with elevated Mg, Mn or Al values were eliminated from the area
208 selected for integration.

209 Seawater samples from the Zoo's aquarium were measured in duplicate using a sector field-
210 ICP-MS (Element2, Thermo Scientific). The ICP-MS was run in low resolution mode (24
211 cycles) for ^{138}Ba and in medium resolution (24 cycles) for ^{43}Ca . Calibration was performed
212 through an external calibration series with increasing concentrations of Ba.

213

214 **3 Results**

215 *3.1 Test diameter increase*

216 Average shell diameters increased considerably during the experimental period (Figure 1).
217 Overall, increase in shell diameter did not significantly differ between treatments. Treatment C
218 (seawater Ba/Ca = 64 $\mu\text{mol/mol}$) for *A. lessonii*, however, shows somewhat reduced chamber
219 addition rates per incubated specimen. This may be the consequence of slightly higher mortality
220 under these conditions and a relatively high number of specimens that did not add any
221 chambers. Although not systematically investigated, 2 Petri dishes from this treatment
222 contained relatively many bleached (i.e. devoid of symbionts) specimens at the end of the 6-
223 week period.

224

225 *3.2 Barium incorporation*



226 Calcite Ba/Ca increases linearly with seawater Ba/Ca for both species (Figure 2; Table 2).
227 ANOVA performed on the individual data points combined with regression analyses reveals a
228 significant increase of Ba/Ca_{cc} with Ba/Ca_{sw} for both species (Table 3). Calculated regression
229 slopes result in a D_{Ba} of 0.326 (±0.005) for *A. lessonii* and 0.777 (±0.007) for *H. depressa*
230 (Figure 3, solid lines). Regression lines are forced through zero as it seems reasonable to assume
231 that no Ba is incorporated into calcite when the Ba concentration in the seawater is zero.
232 Without this forcing, calculated partition coefficients would be 0.335 (±0.022) for *A. lessonii*
233 and 0.919 (±0.030) for *H. depressa*. The resulting partition coefficients ((Ba/Ca_{cc})/(Ba/Ca_{sw}))
234 are constant and significantly different between the species (ANOVA) (~0.3 for *A. lessonii* and
235 ~0.8 for *H. depressa*) over the range of seawater Ba/Ca studied here. The regression line for
236 Ba/Ca_{cc} as a function of Ba/Ca_{sw} for *A. lessonii* corresponds well with that reported for a number
237 of different low Mg species (Lea and Boyle, 1989).
238 The aquarium-derived specimens (field samples) had an diameter ranging from 550 to 1180 µm
239 (with an average of 975 µm) for *A. lessonii* and from 1380 to 2340 µm (average: 1936 µm) for
240 *H. depressa*. They had an average Ba/Ca of 15.4 (±2.3 SD) µmol/mol for *A. lessonii* and 35.7
241 (±14 SD) µmol/mol for *H. depressa*. In combination with the measured aquarium's seawater
242 Ba/Ca of 35.7 (±3.9 SD) µmol/mol, the partition coefficients for Ba vary between 0.43 and 1.0
243 for *A. lessonii* and *H. depressa*, respectively. Since the conditions in which the specimens from
244 the aquarium were grown, are relatively poorly constrained, they are not used for the regression
245 analysis, but are included (Figure 2) to compare with the cultured specimens.

246

247 3.3 Intrachamber variability in Ba/Ca

248 From both species, 10 specimens were used to quantify the relation between ontogeny (i.e. size-
249 dependent) and Ba incorporation into foraminiferal calcite. For this purpose, the final 6-7
250 chambers of these individuals were ablated (Figure 3). With the selected spot diameter (80 µm),



251 ablation of a small amount of material of adjacent chambers could not always be avoided. Some
252 chamber walls, particularly of the youngest (i.e. built latest) chambers, were too thin for reliable
253 measurements and were excluded from further analysis.

254 Since these specimens were cultured at different Ba/Ca_{sw} , the inter-chamber variability is
255 expressed as the difference of a single-chamber Ba/Ca and the individual's average Ba/Ca .

256 Positive single-chamber values indicate higher than average values, whereas negative values
257 indicate single-chamber Ba/Ca below that individual's average Ba/Ca (Figure 3).

258

259 In *H. depressa*, Ba/Ca_{cc} increases significantly with subsequent chamber addition (Figure 3).

260 Regression analysis reveals an average decrease of $1.43 \mu\text{mol/mol}$ Ba/Ca_{cc} per chamber (Table
261 4). Ba/Ca_{cc} appears to decrease with chamber position in *A. lessonii*, although the ANOVA p-
262 value shows that this is statistically not significant. Still, removing one single outlier already
263 results in a p-value lower than 0.01. This implies that the current data set does not allow
264 rejecting the presence of a trend for *A. lessonii*.

265

266 3.4 Relation between incorporation of barium and magnesium

267 The species-specific single-chamber Mg/Ca and Ba/Ca combined for all treatments are
268 positively and significantly related (Figure 4). For *A. lessonii*, $Mg/Ca = 3.1 * Ba/Ca - 3.6$ (t-
269 value = 12.2, $p < 0.01$ for the slope of the regression) and for *H. depressa*, $Mg/Ca = 1.1 * Ba/Ca$
270 $+ 92$ (t-value = 14.8, $p < 0.01$ for the slope). The slopes of these two regressions (3.1 and 1.1)
271 are significantly different: this is calculated by $z = (a_{Heterostegina} - a_{Amphistegina}) / \sqrt{(SE_{a,Heterostegina}^2 +$
272 $SE_{a,Amphistegina}^2)}$, where a is the value for the regression's slope and SE_a is the slope's associated
273 standard error. For the slopes of the Mg/Ca - Ba/Ca regressions for *Amphistegina* and
274 *Heterostegina*, the resulting in a z-score is higher than >7 , indicating that the two slopes are



275 significantly different. When combining the data from both species, the regression is
276 represented by: $Mg/Ca = 2.5 * Ba/Ca + 16$ (t-value = 31.4, $p < 0.01$ for the slope).

277 When comparing the single-chamber D_{Ba} with D_{Mg} , of all data combined, the partition
278 coefficient for Mg is over 30 times lower than that of for Ba (Figure 4). Over the range in
279 Ba/Ca_{sw} studied here, the relation between D_{Ba} and D_{Mg} is linear within both species. For *A.*
280 *lessonii*, $D_{Mg} = 40 * D_{Ba} - 2.0$ (t-value = 7.3, $p < 0.01$ for the slope of the regression) and for *H.*
281 *depressa*, $D_{Mg} = 29 * D_{Ba} + 3.8$ (t-value = 6.5, $p < 0.01$ for the slope). The slopes of these two
282 regressions (40 and 29) are not significantly different (z-score 1.6). When combining the data
283 from both species, the regression equals: $D_{Mg} = 34 * D_{Ba} + 0.073$ (t-value = 29.9, $p < 0.01$ for the
284 slope).

285

286 **4 Discussion**

287 *4.1 Test diameter increase*

288 The range of Ba concentrations used in the experiments did not influence the increase in shell
289 diameter of either foraminiferal species (Figure 1). Compared to *H. depressa*, increases in shell
290 diameter (which is proportional to the chamber addition rate) for *A. lessonii* were slightly more
291 variable. To prevent barite precipitation it was necessary to reduce the sulphate concentration
292 below that typically measured in natural seawater. Sulphate concentrations between 0.1 and 1
293 mmol/L do not affect inorganic calcite growth (Reddy and Nancollas, 1976), but a decrease in
294 growth rates of approximately 30% was observed in coccolithophores growing in artificial
295 seawater with a sulphate concentration 10% that of natural seawater (Langer et al., 2009).
296 Although coccolithophores and foraminifera may respond differently to lowered sulphate
297 concentrations, this reduction could have hampered growth of the specimens in our culturing
298 experiment. Chamber addition rates of *A. lessonii* in a culture set-up with a sulphate
299 concentrations similar to that of natural seawater (Mewes et al., 2014) were approximately 20%



300 higher than chamber addition rates observed in our experiments. Since these experiments were
301 not performed simultaneously using specimens from the same batch, it is not straight forward
302 to compare absolute rates and therefore the 20% difference cannot unambiguously be attributed
303 to sulphate concentration (Hoppe et al. 2011). Unfortunately no data exist on the effect of
304 reduced sulphate concentrations on the uptake of trace elements in foraminiferal calcite.
305 However Langer et al. (2009) demonstrated that sulphate limitation had no discernible effect
306 on Ba incorporation in coccolithophore calcite.

307

308 *4.2 Barium incorporation*

309 The variability in Ba/Ca between individual ablation craters is considerable, but the average
310 foraminiferal Ba/Ca shows a consistent relation with seawater Ba/Ca. This implies that the
311 observed variability is a reflection of the inhomogeneous distribution in the test and hence
312 filtered out when averaging. This is similar to the behavior for Mg and Sr (Sadekov et al., 2008;
313 Wit et al., 2012; De Nooijer et al., 2014a) and underscores the power of single-chamber
314 analyses. If present, inhomogeneity in test wall Ba/Ca in combination with different cross
315 section sampled during the ablation potentially account for the observed variability. This would
316 imply that although large differences are observed within a test wall, the average still reliably
317 reflects sea water concentration (this paper) and for Mg, still reflects seawater temperature
318 (Hathorne et al., 2009). Comparing within-specimen and between-specimen variability, De
319 Nooijer et al. (2014a) showed that within specimen variability does not account for the complete
320 observed variability for Mg/Ca in *Ammonia tepida*. This seems to be similar for Ba/Ca
321 (compare Figure 4 in this paper with Figure 5 from De Nooijer et al., 2014a), which would
322 mean that on average 20 chambers need to be analyzed to reach a 5% relative precision (De
323 Nooijer et al., 2014a). This is not limited by the analytical precision, but rather due to inherent



324 biological inter-chamber and inter-specimen variability. To reduce ontogenetic variability, a
325 narrow size fraction should be analyzed.

326 Incorporation of Ba in *H. depressa* shows a partitioning which is about 2.5 times higher than in
327 *A. lessonii*. Such a large offset of D_{Ba} between benthic species has not been observed before.
328 Lea and Boyle (1989) found $D_{Ba} = 0.37 \pm 0.06$ for *Cibicidoides wuellerstorfi*, *Cibicidoides*
329 *kullenbergi* and *Uvigerina* spp. for a series of core tops, comparable to the partition coefficient
330 reported here for *A. lessonii* (0.33 ± 0.022 ; Figure 2). In contrast, partition coefficients for Ba
331 in planktonic foraminifera are roughly only twice as low as these benthic foraminiferal
332 partitioning coefficients (0.14-0.19; Hönisch et al., 2011; Lea and Boyle, 1991; Lea and Spero,
333 1992). Although temperature, pH, salinity and pressure were initially proposed as potential
334 explanation for the offset between planktonic and benthic D_{Ba} (Lea and Boyle, 1991; Lea and
335 Spero, 1992), studies by Lea and Spero (1994) and Hönisch et al. (2011) showed no significant
336 impact of temperature, pH and salinity on Ba incorporation into planktonic foraminiferal
337 calcite. This would leave hydrostatic pressure to explain the difference between benthic and
338 planktonic species. Our observations show, however, that the observed differences in D_{Ba}
339 between *H. depressa* and *A. lessonii* and also the offset with the planktonic species are inherent
340 to these species. There may be a small impact of environmental parameters, explaining the
341 slightly higher partition coefficients for Ba in the “field” specimens taken from the aquarium
342 compared to the cultured ones (Figure 2). The overall differences in partitioning seem to
343 coincide with different taxonomic groups, which may indicate that foraminifera may differ in
344 their controls on transporting ions from seawater to the site of calcification. For example, the
345 contribution of transmembrane transport versus that of seawater transport (i.e. leakage; Nehrke
346 et al., 2013 or vacuolization; Erez, 2003) may vary between species and thereby account for
347 differences in Mg/Ca, Ba/Ca, etc. (Nehrke et al., 2013).



348

349 *4.3 Inter-chamber variability of Ba/Ca_{cc}*

350 In both species cultured here, Ba/Ca_{cc} decreases significantly from largest (i.e. built latest in
351 life) towards the smaller chambers (Figure 3). Observed trends were not significantly different
352 between *A. lessonii* and *H. depressa*, suggesting that Ba/Ca_{cc} decreases at the same rate with
353 size, despite the overall difference in Ba/Ca_{cc} (Figure 3). Since we always analyzed chambers
354 at the same position (F-1 for *A. lessonii* and F-2 for *H. depressa*) and since the final size of the
355 cultured specimens was similar between treatments (Figure 1), ontogenetic trends in Ba/Ca do
356 not influence the trends in Ba/Ca between treatments (Figure 2). Several other studies showed
357 that element/Ca ratios can vary with chamber position. Raitzsch et al. (2011), for example,
358 reported increasing B/Ca and decreasing Mg/Ca towards younger chambers in the benthic
359 *Planulina wuellerstorfi*. Such patterns maybe related to changes in the surface-to-volume ratio
360 or relative changes “vital effects” as foraminifera grow larger. For example, pH reduction in
361 the foraminiferal microenvironment is related to the specimen’s size (Glas et al., 2012) and may
362 thereby affect the chemical speciation of minor and trace element, which in turn, may determine
363 their uptake rates. Hönisch et al. (2011), however, showed that seawater pH has no noticeable
364 effect on Ba incorporation in planktonic foraminiferal calcite, rendering changes in the pH of
365 the foraminiferal microenvironment an unlikely explanation to account for the observed
366 chamber-to-chamber variability in Ba/Ca. Alternatively, changes in the metabolic rate, the
367 instantaneous calcification rate, or a different partitioning between the impacts of the life
368 processes may lead to the observed ontogenetic trend.

369 Bentov and Erez (2006) argued that decreasing Mg/Ca with foraminifera test size could be
370 explained by relatively high Mg-concentrations at or near the primary organic sheet (POS),
371 which is the organic matrix on which the first layer of calcite precipitates during the formation
372 of a new chamber. With the formation of a new chamber, a low-Mg calcite layer is deposited



373 over all existing chambers, so that the high-Mg phase is being ‘diluted’ as more layers are
374 deposited (Bentov and Erez, 2006). Future studies may indicate whether Ba/Ca is also
375 heterogeneously distributed within chamber walls, by for example, being enriched close to the
376 POS (Kunioka et al., 2006). If this is the case, lamellar calcification mode may also result in
377 changing Ba/Ca with chamber position.

378

379 *4.4 Coupled incorporation of barium and magnesium*

380 If incorporation of Ba and Mg (and Na, Sr and B) are physically linked during
381 biomineralization, inter-species differences in composition may likely be correlated across the
382 various elements. The correlation between Mg/Ca and Ba/Ca within and between species
383 (Figure 4) suggests that these two elements are simultaneously affected during their
384 incorporation. The relationship between Mg/Ca and Ba/Ca is different between the two species,
385 which may be (partly) caused by the variability in seawater chemistry between treatments (i.e.
386 seawater Ba/Ca and Mg/Ca; Table 1). Alternatively, incorporation of Mg in *H. depressa* may
387 be close to the maximum concentration of Mg that can be incorporated into a calcite crystal
388 lattice at ambient conditions (Morse et al., 2007). This may result in an overall asymptotic
389 relationship between Mg/Ca and Ba/Ca as Mg/Ca approaches ~200 mmol/mol (Figure 4).

390 When correcting for the different seawater Ba/Ca and Mg/Ca between treatments, incorporated
391 Ba and Mg correlate similarly within, as well as, between the two species studied here (Figure
392 4). This suggests that these elements are coupled during biomineralization and that the ratio of
393 Ba and Mg in seawater is preserved during calcification by these species of foraminifera. When
394 comparing the relation between Ba/Ca and Mg/Ca from other benthic species (e.g. Lea and
395 Boyle, 1989; figure 2; more refs), the coupling between Ba- and Mg-incorporation is likely
396 similar across a wide range of benthic foraminiferal species.

397

398 *4.5 Biomineralization and element incorporation*

399 Foraminiferal biomineralization determines incorporation of many elements and fractionation
400 of many isotopes during the production of new chamber as indicated by overall large
401 compositional differences between inorganically precipitated and foraminiferal calcite (Erez,
402 2003; Bentov and Erez, 2006; Nehrke et al., 2013; De Nooijer et al., 2014b). For example,
403 Mg/Ca ratios in many species are orders of magnitude lower than what is expected from
404 inorganic precipitation experiments. Additionally, Mg/Ca varies considerably between
405 foraminiferal species and especially between species known to have different calcification
406 strategies (Bentov and Erez, 2006; Toyofuku et al., 2011; Wit et al., 2012; De Nooijer et al.,
407 2009; 2014b). Other elements such as Sr (e.g. Elderfield et al., 2000) and B/Ca (e.g. Allen et
408 al., 2012) also vary significantly between species. Generally, concentrations for these elements
409 correlate within taxa and hence species incorporating relatively much Mg, also have high (for
410 example) Sr/Ca, B/Ca and Na/Ca. Miliolids and many ‘Large Benthic Foraminifera’ (LBF)
411 produce calcite with Mg/Ca up to 100-150 mmol/mol (Toyofuku et al., 2000; Dueñas-
412 Bohórquez et al., 2011; Sadekov et al., 2014; Evans et al., 2015), while most planktonic and
413 symbiont-barren benthic foraminifera produce test calcite with Mg/Ca values ranging from 1-
414 10 mmol/mol (e.g. Nürnberg et al., 1996; Elderfield et al., 2002; Lear et al., 2010; Wit et al.,
415 2012; De Nooijer et al., 2014b). The same distinction is observed for B/Ca (compare e.g. Allen
416 et al., 2012 and Kazcmarek et al., 2015), Li/Ca (Lear et al., 2010 versus Evans et al., 2015),
417 Na/Ca (Wit et al., 2013 versus Evans et al., 2015) and Sr/Ca (e.g. Dueñas-Bohórquez et al.,
418 2011). The correlation between relatively high (for example) Mg/Ca, Sr/Ca and B/Ca
419 corresponds to the observed trends in the data presented here for Ba/Ca and Mg/Ca in *H.*
420 *depressa* and *A. lessonii* (Figure 4). The Mg/Ca in the former species is approximately 2.5 times
421 that of the latter, which is similar to the difference in Ba/Ca ratios between these species and
422 implies that Ba changes in concert with Mg, which is consistent with the single-chamber



423 correlation between Mg/Ca and Ba/Ca (Figure 4). Although such a change could potentially be
424 caused inorganically by differences in Mg opening up the crystal lattice in such a way that it
425 can accommodate more or less Ba. Such a mechanism is described for Mg and Sr (e.g. Morse
426 and Bender, 1990; Mucci and Morse, 1983; Mewes et al., 2015; Langer et al., 2016) and may
427 also apply to Ba incorporation and the influence of Mg ions that increase stress in the calcite
428 crystal lattice. However, such a mechanism is unlikely a sufficient explanation, since it is
429 observed that Ba incorporation does not change in the planktonic *Orbulina universa* cultured at
430 temperatures from 18 and 26 °C (Hönisch et al., 2011), even though this temperature range
431 roughly doubles the shell's Mg/Ca (Lea et al., 1999). Unless the strain of incorporated Mg ions
432 does not increase linearly with its concentration, the covariance between Mg and in this case
433 Ba may well be interrelated during an earlier stage of the biomineralization process, e.g. during
434 their transport from the surrounding seawater into the site of calcification (Erez, 2003; De
435 Nooijer et al., 2014b).

436 Interestingly, the partitioning of different elements is not the same between taxa. For example,
437 Sr/Ca in LBFs is approximately twice as high (Dueñas-Bohorquez et al., 2011; Evans et al.,
438 2015) as in planktonic species (Elderfield et al., 2002; Dueñas-Bohórquez et al., 2009; Hendry
439 et al., 2009), whereas the ratio between the D_{Mg} of these groups is between 10 and 100 (see
440 above). Comparing the offset of D between groups as a function of D itself shows an
441 approximate logarithmic correlation (Figure 5). The distinction between the two groups on basis
442 of their element signature coincides with known differences in biomineralization controls.
443 Element controls in low-Mg species are thought to be determined by (highly) selective trans-
444 membrane ion transporters, (limited) leakage of seawater into the site of calcification and/or
445 selective Mg^{2+} -removal (Nehrek et al., 2013; De Nooijer et al., 2014b). Miliolid foraminifera
446 belong to the high-Mg foraminiferal group and are known to secrete their calcite intracellularly
447 (Hemleben et al., 1986; Ter Kuile and Erez, 1991; De Nooijer et al., 2009). These intracellular



448 vesicles may be derived from endocytosed seawater and therefore contain relatively high
449 concentrations of Mg^{2+} , Ba^{2+} and other ions present in seawater, although so far only Sr/Ca and
450 Mg/Ca of Miliolid foraminifera have been published (supplementary information). The
451 biomineralization of non-Miliolid, intermediate- and high-Mg benthic foraminifera may
452 employ characteristics of both these types of calcification and therefore incorporate moderately
453 to high concentrations of elements (cf Segev and Erez, 2006).

454

455 5 Conclusions

456 Results from this study indicate that differences in D_{Ba} between species of foraminifera are
457 larger than previously thought. This implies that species-specific Ba partition coefficients need
458 to be applied to reconstruct past Ba/Ca_{sw} and/or salinity (Lea and Boyle, 1989; Weldeab et al.,
459 2007). Moreover, our results underscore the necessity to account for size-related effects on
460 Ba/Ca_{cc}. This effect may bias obtained Ba/Ca_{cc} particularly when using single chamber
461 measurements. When determining Ba/Ca_{cc} by dissolution of whole shells, the contribution of
462 smaller chambers (with lower Ba/Ca_{cc}) is relatively small compared to a specimen's overall
463 Ba/Ca and thus does not affect average values. Our results also show that within species as well
464 as between species, single-chambered Mg/Ca and Ba/Ca are linearly correlated. The difference
465 in Ba/Ca between the two species studied here fits with previously observed variability in
466 element/Ca ratios between foraminifera taxa and may correspond to differences in their
467 biomineralization mechanisms.

468

469 References

470 Allen, K.A., Hönisch, B., Eggins, S.M., Yu, J., Spero, H.J., Elderfield, H., 2011. Controls on
471 Boron incorporation in cultured tests of the planktic foraminifer *Orbulina universa*.
472 Earth Planet. Sci. Lett. 309, 291-301.



- 473 Allen, K.A., Hönisch, B., Eggins, S.M., Rosenthal, Y., 2012. Environmental controls on B/Ca
474 in calcite tests of the tropical planktic foraminifer species *Globigerinoides ruber* and
475 *Globigerinoides sacculifer*. Earth Planet. Sci. Lett. 351-352, 270-280.
- 476 Babila, T.L., Rosenthal, Y., Conte, M.H., 2014. Evaluation of the biogeochemical controls on
477 B/Ca of *Globigerinoides ruber* from the Ocean Flux Program, Bermuda. Earth Planet.
478 Sci. Lett. 404, 67-76.
- 479 Bahr, A., Schönfeld, J., Hoffmann, J., Voigt, S., Aurahs, R., Kucera, M., Slögel, S., Jentzen,
480 A., Gerdes, A., 2013. Comparison of Ba/Ca and $\delta^{18}\text{O}_{\text{water}}$ as freshwater proxies: A
481 multi-species core-top study on planktonic foraminifera from the vicinity of the
482 Orinoco River mouth. Earth Planet. Sci. Lett. 383, 45-57.
- 483 Bentov, S., Erez, J., 2006. Impact of biomineralization processes on the Mg content of
484 foraminiferal shells: A biological perspective. Geochem. Geophys. Geosyst. 7,
485 Q01P08.
- 486 Bian, N., Martin, P.A., 2010. Investigating the fidelity of Mg/Ca and other element data from
487 reductively cleaned planktonic foraminifera. Paleocyanography 25, PA2215.
- 488 Boyle, E.A., 1981. Cadmium, zinc, copper and barium in foraminifera tests. Earth Planet. Sci.
489 Lett. 53, 11-35.
- 490 Bradshaw, A.L., Brewer, P.G., Shafer, D.K., Williams, R.T., 1981. Measurements of total
491 carbon dioxide and alkalinity by potentiometric titration in the GEOSECS program.
492 Earth Planet. Sci. Lett. 55, 99-115.
- 493 Bryan, S.P., Marchitto, T.M., 2008. Mg/Ca-temperature proxy in benthic foraminifera: New
494 calibrations from the Florida Straits and a hypothesis regarding Mg/Li.
495 Paleocyanography 23, PA2220.



- 496 Dawber, C.F., Tripathi, A., 2012. Relationships between bottom water carbonate saturation and
497 element/Ca ratios in coretop samples of the benthic foraminifera *Oridorsalis*
498 *umbonatus*. Biogeosciences 9, 3029-3045.
- 499 De Nooijer, L.J., Toyofuku, T., Kitazato, H., 2009. Foraminifera promote calcification by
500 elevating their intracellular pH. Proc. Natl. Acad. Sci. USA 106, 15374-15378.
- 501 De Nooijer, L.J., Hathorne, E.C., Reichart, G.J., Langer, G., Bijma, J., 2014a. Variability in
502 calcitic Mg/Ca and Sr/Ca ratios in clones of the benthic foraminifer *Ammonia tepida*.
503 Marine Micropaleontology 107, 33-43.
- 504 De Nooijer, L.J., Spero, H.J., Erez, J., Bijma, J., Reichart, G.J., 2014b. Biomineralization in
505 perforate foraminifera. Earth-Sci. Rev. 135, 48-58.
- 506 Dickson, A.G., Millero, F.J., 1987. A comparison of the equilibrium constants for dissociation
507 constants of carbonic acid in seawater media. Deep Sea Res. 34, 1733-1743.
- 508 Dueñas-Bohórquez, A., Da Rocha, R., Kuroyanagi, A., Bijma, J., Reichart, G.J., 2009. Effect
509 of salinity and seawater calcite saturation state on Mg and Sr incorporation in cultured
510 planktonic foraminifera. Marine Micropaleontology 73, 178-189.
- 511 Dueñas-Bohórquez, A., Raitzsch, M., De Nooijer, L.J., Reichart, G.J., 2011. Independent
512 impacts of calcium and carbonate ion concentration on Mg and Sr incorporation in
513 cultured benthic foraminifera. Marine Micropaleontology 81, 122-130.
- 514 Eggins, S., De Deckker, P., Marshall, J., 2003. Mg/Ca variation in planktonic foraminifera tests:
515 implications for reconstructing palaeo-seawater temperature and habitat migration.
516 Earth Planet. Sci. Lett. 212, 291-306.
- 517 Elderfield, H., Cooper, M., Ganssen, G., 2000. Sr/Ca in multiple species of planktonic
518 foraminifera: Implications for reconstructions of seawater Sr/Ca. Geochem. Geophys.
519 Geosyst. 1, GC000031.



- 520 Elderfield, H., Vautravers, M., Cooper, M., 2002. The relationship between shell size and
521 Mg/Ca, Sr/Ca, $\delta^{18}\text{O}$, and $\delta^{13}\text{C}$ of species of planktonic foraminifera. *Geochem.*
522 *Geophys. Geosyst.* 3, GC000194.
- 523 Elderfield, H., Yu, J., Anand, P., Kiefer, T., Nyland, B., 2006. Calibrations for benthic
524 foraminiferal Mg/Ca paleothermometry and the carbonate ion hypothesis. *Earth*
525 *Planet. Sci. Lett.* 250, 633-649.
- 526 Erez, J., 2003. The source of ions for biomineralization in foraminifera and their implications
527 for paleoceanographic proxies. *Rev. Mineral. Geochem.* 54, 115-149.
- 528 Evans, D., Erez, J., Oron, S., Müller, W., 2015. Mg/Ca-temperature and seawater-test chemistry
529 relationships in the shallow-dwelling large benthic foraminifera *Operculina*
530 *ammonoides*. *Geochim. Cosmochim. Acta* 148, 325-342.
- 531 Foster, G.L., 2008. Seawater pH, $p\text{CO}_2$ and $[\text{CO}_3^{2-}]$ variations in the Caribbean Sea over the
532 last 130 kyr: A boron isotope and B/Ca study of planktonic foraminifera. *Earth and*
533 *Planetary Science Letters* 271, 254-266.
- 534 Glas, M.S., Langer, G., Keul, N., 2012. Calcification acidifies the microenvironment of a
535 benthic foraminifer (*Ammonia* sp.). *J. Exp. Mar. Biol. Ecol.* 424-425, 53-58.
- 536 Gran, G., 1952. Determination of the equivalence point in potentiometric titrations-- Part II.
537 *The Analyst* 77, 661-671.
- 538 Guillong, M., Meier, D.L., Allan, M.M., Heinrich, C.A., Yardley, B.W.D., 2008. SILLS: A
539 MATLAB-based program for the reduction of laser ablation ICP-MS data of
540 homogeneous materials and inclusions. *Mineralogical Association of Canada Short*
541 *Course* 40, 328-333.
- 542 Hall, J.M., Chan, L.-H., 2004a. Li/Ca in multiple species of benthic and planktonic
543 foraminifera: Thermocline, latitudinal, and glacial-interglacial variation. *Geochim.*
544 *Cosmochim. Acta* 68, 529-545.



- 545 Hall, J.M., Chan, L.-H., 2004b. Ba/Ca in *Neogloboquadrina pachyderma* as an indicator of
546 deglacial meltwater discharge into the western Arctic Ocean. *Paleoceanography* 19,
547 PA000910.
- 548 Hathorne, E.C., James, R.H., Savage, P., Alard, O., 2008. Physical and chemical characteristics
549 of particles produced by laser ablation of biogenic calcium carbonate. *J. Anal. Atom.*
550 *Spectrom.* 23, 240-243.
- 551 Hathorne, E.C., James, R.H., Lampitt, R.S., 2009. Environmental versus biomineralization
552 controls on the intratest variation in the trace element composition of the planktonic
553 foraminifera *G. inflata* and *G. scitula*. *Paleoceanography* 24, PA001742.
- 554 Hemleben, C., Anderson, O.R., Berthold, W., Spindler, M., 1986. Calcification and chamber
555 formation in foraminifera - an overview. pp 237-249. In: *Biomineralization in lower*
556 *plants and animals*, Leadbeater, B.S.C. and Riding, R. (eds) The Systematics Society,
557 London.
- 558 Hendry, K.R., Rickaby, R.E.M., Meredith, M.P., Elderfield, H., 2009. Controls on stable
559 isotope and trace metal uptake in *Neogloboquadrina pachyderma* (sinistral) from an
560 Antarctic sea-ice environment. *Earth Planet. Sci. Lett.* 278, 67-77.
- 561 Hoffmann, J., Bahr, A., Voigt, S., Schönfeld, J., Nürnberg, D., Rethemeyer, J., 2014.
562 Disentangling abrupt deglacial hydrological changes in northern South America:
563 Insolation versus oceanic forcing. *Geology* 42, 579-582.
- 564 Hönisch, B., Allen, K.A., Russell, A.D., Eggins, S.M., Bijma, J., Spero H.J., Lea, D.W., Yu, J.,
565 2011. Planktic foraminifers as recorders of seawater Ba/Ca. *Marine*
566 *Micropaleontology* 79, 52-57.
- 567 Hoppe, C.J.M., Langer, G., Rost, B., 2011. *Emiliana huxleyi* shows identical responses to
568 elevated pCO₂ in TA and DIC manipulations. *J. Exp. Mar. Biol. Ecol.* 406, 54–62.



- 569 Jochum, K.P., Weis, U., Stoll, B., Kuzmin, D., Yang, Q., Raczek, I., Jacob, D.E., Stracke, A.,
570 Birbaum, K., Frick, D.A., Günther, D., Enzweiler, J., 2011. Determination of
571 reference values for NIST SRM 610-617 glasses following ISO guidelines. *Geostand.*
572 *Geoanal. Res.* 35, 397-429.
- 573 Kaczmarek, K., Langer, G., Nehrke, G., Horn, I., Misra, S., Janse, M., Bijma, J., 2015. Boron
574 incorporation in the foraminifer *Amphistegina lessonii* under a decoupled carbon
575 chemistry. *Biogeosciences* 12, 1753-1763.
- 576 Kester, D.R., Duedall, I.W., Connors, D.N., 1967. Preparation of artificial seawater. *Limnol.*
577 *Oceanogr.* 12, 176-179.
- 578 Kunioka, D., Shirai, K., Takahata, N., Sano, Y., Toyofuku, T., Ujiie, Y., 2006.
579 Microdistribution of Mg/Ca, Sr/Ca, and Ba/Ca ratios in *Pulleniatina obliquiloculata*
580 test by using a NanoSIMS: Implication for the vital effect mechanism. *Geochem.*
581 *Geophys. Geosyst.* 7, GC001280.
- 582 Langer, G., Nehrke, G., Thoms, S., Stoll, H., 2009. Barium partitioning in coccoliths of
583 *Emiliania huxleyi*. *Geochim. Cosmochim. Acta* 73, 2899-2906.
- 584 Langer G., Sadekov, A., Thoms, S., Keul, N., Nehrke, G., Mewes, A., Greaves, M., Misra, S.,
585 Reichart, G.J., De Nooijer, L.J., Bijma, J., Elderfield, H., 2016. Sr partitioning in the
586 benthic foraminifera *Ammonia aomoriensis* and *Amphistegina lessonii*. *Chemical*
587 *Geology* 440: 306-312.
- 588 Lea, D.W., 1995. A trace metal perspective on the evolution of Antarctic circumpolar deepwater
589 chemistry. *Paleoceanography* 10, 733-747.
- 590 Lea, D., Boyle, E., 1989, Barium content of benthic foraminifera controlled by bottom-water
591 composition. *Nature* 338, 751-753.
- 592 Lea, D.W., Boyle, E.A., 1990. A 210,000-year record of barium variability in the deep
593 northwest Atlantic Ocean. *Nature* 347, 269-272.



- 594 Lea, D.W., Boyle, E.A. 1991. Barium in planktonic foraminifera. *Geochim. Cosmochim. Acta*
595 55, 3321-3331.
- 596 Lea, D.W., Boyle, E.A., 1993. Determination of carbonate-bound barium in foraminifera and
597 corals by isotope dilution plasma-mass spectrometry. *Chem. Geol.* 103, 73-84.
- 598 Lea, D.W., Spero, H.J., 1992. Experimental determination of barium uptake in shells of the
599 planktonic foraminifera *Orbulina universa* at 22° C. *Geochim. Cosmochim. Acta* 56,
600 2673-2680.
- 601 Lea, D.W., Spero, H.J., 1994. Assessing the reliability of paleochemical tracers: Barium uptake
602 in the shells of planktonic foraminifera. *Paleoceanography* 9, 445-452.
- 603 Lea, D.W., Mashiotto, T.A., Spero, H.J., 1999. Controls on magnesium and strontium uptake
604 in planktonic foraminifera determined by live culturing. *Geochim. Cosmochim. Acta*
605 63, 2369-2379.
- 606 Lear, C.H., Mawbey, E.M., Rosenthal, Y., 2010. Cenozoic benthic foraminiferal Mg/Ca and
607 Li/Ca records: Toward unlocking temperatures and saturation states.
608 *Paleoceanography* 25, PA001880.
- 609 Lee, J.J., 2006. Algal symbiosis in larger foraminifera. *Symbiosis* 42, 63-75.
- 610 Lewis, E., Wallace, D., 1998. Program developed for CO₂ system calculations, p 38.
- 611 Marr, J.P., Carter, L., Bostock, H.C., Bolton, A., Smith, E., 2013. Southwest Pacific Ocean
612 response to a warming world: Using Mg/Ca, Zn/Ca, and Mn/Ca in foraminifera to
613 track surface ocean water masses during the last deglaciation. *Paleoceanography* 28,
614 347-362.
- 615 Marriott, C.S., Henderson, G.M., Crompton, R., Staubwasser, M., Shaw, S., 2004. Effect of
616 mineralogy, salinity, and temperature on Li/Ca and Li isotope composition of calcium
617 carbonate. *Chemical Geology* 212, 5-15.



- 618 Mehrbach, C., Culberson, C.H., Hawley, J.E., Pytkowicz, R.N., 1973. Measurement of the
619 apparent dissociation constants of carbonic acid in seawater at atmospheric pressure.
620 *Limnol. Oceanogr.* 18, 897-907.
- 621 Mewes, A., Langer, G., De Nooijer, L.J., Bijma, J., Reichart, G.J., 2014. Effect of different
622 seawater Mg^{2+} concentrations on calcification in two benthic foraminifers. *Marine*
623 *Micropaleontology* 113, 56-64.
- 624 Mewes, A., Langer, G., Reichart, G.J., De Nooijer, L.J., Nehrke, G., Bijma, J., 2015. The impact
625 of Mg contents on Sr partitioning in benthic foraminifers. *Chem. Geol.* 412, 92-98.
- 626 Morse, J.W., Bender, M.L., 1990. Partition coefficients in calcite: Examination of factors
627 influencing the validity of experimental results and their application to natural systems.
628 *Chem. Geol.* 82, 265-277.
- 629 Morse, J.W., Arvidson, R.S., Lüttge, A., 2007. Calcium carbonate formation and dissolution.
630 *Chem. Rev.* 107: 342-381.
- 631 Mucci, A., Morse, J.W., 1983. The incorporation of Mg^{2+} and Sr^{2+} into calcite overgrowths:
632 influences of growth rate and solution composition. *Geochim. Cosmochim. Acta* 47,
633 217-233.
- 634 Nehrke, G., Keul, N., Langer, G., De Nooijer, L.J., Bijma, J., Meibom, A., 2013. A new model
635 for biomineralization and trace-element signatures of foraminifera tests.
636 *Biogeosciences* 10, 6759-6767.
- 637 Ni, Y., Foster, G.L., Bailey, T., Elliott, T., Schmidt, D.N., Pearson, P., Haley, B., Coath, C.,
638 2007. A core top assessment of proxies for the ocean carbonate system in surface-
639 dwelling foraminifera. *Paleoceanography* 22, PA3212.
- 640 Nürnberg, D., Bijma, J., Hemleben, C., 1996. Assessing the reliability of magnesium in
641 foraminiferal calcite as a proxy for water mass temperatures. *Geochim. Cosmochim.*
642 *Acta* 80, 803-814.



- 643 Okai, T., Suzuki, A., Kawahata, H., Terashima, S., Imai, N., 2002. Preparation of a New
644 Geological Survey of Japan Geochemical Reference Material: Coral JCp-1,
645 Geostandards Newsletter 26, 95-99.
- 646 Pak, D.K., Lea, D.W., Kennett, J.P., 2004. Seasonal and interannual variation in Santa Barbara
647 Basin water temperatures observed in sediment trap foraminiferal Mg/Ca. *Geochem.*
648 *Geophys. Geosyst.* 5, Q12008.
- 649 Pierrot, D., Lewis, E., Wallace, D.W.R., 2006. MS Excel program developed for CO₂ system
650 calculations. ORNL/CDIAC-105. Carbon dioxide Information Analysis Center, Oak
651 Ridge National Laboratory, US department of Energy, Oak Ridge, Tennessee.
- 652 Raitzsch, M., Hathorne, E.C., Kuhnert H., Groeneveld, J., Bickert, T., 2011. Modern and late
653 Pleistocene B/Ca ratios of the benthic foraminifer *Planulina wuellerstorfi* determined
654 with laser ablation ICP-MS. *Geology* 39, 1039-1042.
- 655 Raja, R., Saraswati, P.K., Rogers, K., Iwao, K., 2005. Magnesium and strontium compositions
656 of recent symbiont-bearing benthic foraminifera. *Marine Micropaleontology* 58, 31-
657 44.
- 658 Reddy, M.M., Nancollas, G.H., 1976. The crystallization of calcium carbonate: IV. The effect
659 of magnesium, strontium and sulfate ions. *J. Crystal Growth* 35, 33-38.
- 660 Reichart, G.J., Jorissen, F., Anschutz, P., Mason, P.R.D., 2003. Single foraminiferal test
661 chemistry records the marine environment. *Geology* 31, 355-358.
- 662 Sadekov, A., Eggins, S.M., De Deckker, P., Kroon, D., 2008. Uncertainties in seawater
663 thermometry deriving from intratest and intertest Mg/Ca variability in *Globigerinoides*
664 *ruber*. *Paleoceanography* 23, PA0014502.
- 665 Sadekov, A., Bush, F., Kerr, J., Ganeshram, R., Elderfield, H., 2014. Mg/Ca composition of
666 benthic foraminifera *Miliolacea* as a new tool of paleoceanography. *Paleoceanography*
667 29, 990-1001.



- 668 Segev, E., Erez, J., 2006. Effect of Mg/Ca ratio in seawater on shell composition in shallow
669 benthic foraminifera. *Geochem. Geophys. Geosyst.* 7, GC000969.
- 670 Ter Kuile B.H., Erez, J., 1991. Carbon budgets for two species of benthonic symbiont-bearing
671 foraminifera. *Biological Bulletin* 180, 489-495.
- 672 Toyofuku, T., Kitazato, H., Kawahata, H., 2000. Evaluation of Mg/Ca thermometry in
673 foraminifera: Comparison of experimental results and measurements in nature.
674 *Paleoceanography* 15, 456-464.
- 675 Toyofuku, T., Suzuki, M., Suga, H., Sakai, S., Suzuki, A., Ishikawa, T., De Nooijer, L.J.,
676 Schiebel, R., Kawahata, H., Kitazato, H., 2011. Mg/Ca and $\delta^{18}\text{O}$ in the brackish
677 shallow-water benthic foraminifer *Ammonia 'beccarii'*. *Marine Micropaleontology* 78,
678 113-120.
- 679 Weldeab, S., Lea, D.W., Schneider, R.R., Andersen, N., 2007. 155,000 years of west African
680 monsoon and ocean thermal evolution. *Science* 316, 1303-1307.
- 681 Weldeab, S., Lea, D.W., Oberhänsli, H., Schneider, R.R., 2014. Links between southwestern
682 tropical Indian Ocean SST and precipitation over southeastern Africa over the last 17
683 kyr. *Palaeogeogr. Palaeoclimatol. Palaeoecol.* 410, 200-212.
- 684 Wilson, S. A., Koenig, A. E., Orklid, R., 2008. Development of microanalytical reference
685 material (MACS-3) for LA-ICP-MS analysis of carbonate samples, *Geochimica et*
686 *Cosmochimica Acta Supplement* 72, 1025.
- 687 Wit, J.C., De Nooijer, L.J., Barras, C., Jorissen, F.J., Reichart, G.J., 2012. A reappraisal of the
688 vital effect in cultured benthic foraminifer *Bulimina marginata* on Mg/Ca values:
689 assessing temperature uncertainty relationships. *Biogeosciences* 9, 3693-3704.
- 690 Wit, J.C., De Nooijer, L.J., Wolthers, M., Reichart, G.J., 2013. A novel salinity proxy based on
691 Na incorporation into foraminiferal calcite. *Biogeosciences* 10, 6375-6387.
- 692



693 Yu, J., Day, J., Greaves, M., Elderfield, H., 2005. Determination of multiple element/ calcium
694 ratios in foraminiferal calcite by quadrupole ICP-MS. *Geochemistry, Geophysics,*
695 *Geosystems* 6, Q08P01.

696 Yu, J., Elderfield, H., 2007. Benthic foraminiferal B/Ca ratios reflect deep water carbonate
697 saturation state. *Earth and Planetary Science Letters* 258, 73-86.

698

699 **Tables**

700 *Table 1: measured concentrations of major and minor ions, temperature, salinity and*
 701 *carbonate chemistry in the five culture media (A-E).*

Treatment	A	B	C	D	E
Ba (nmol/kg)	488.5	535.5	611.0	608.4	854.6
Ca (mmol/kg)	9.1	9.5	9.6	9.2	9.3
Ba/Ca _{sw} (mmol/mol)	53.68	56.36	63.64	66.14	91.89
Na (mmol/kg)	402	416	389	383	384
B (mmol/kg)	11	11	12	11	11
K (mmol/kg)	0.40	0.46	0.43	0.43	0.42
Mg (mmol/kg)	55	58	59	53	53
Sr (mmol/kg)	0.11	0.11	0.12	0.11	0.11
Mg/Ca _{sw} (mol/mol)	6.04	6.11	6.15	5.76	5.70
T (°C)	25	25	25	25	25
Salinity	32.4	32.4	32.4	32.4	32.4
TA (µmol/kg)	2445	2450	2662	2437	2429
DIC (µmol/kg)	2244 ± 3	2246 ± 6	2464 ± 7	2236 ± 7	2228 ± 9
Ω _{calcite}	3.9	3.9	4.0	3.9	3.9

702

703 *Table 2. Measured Ba/Ca and Mg/Ca for A. lessonii and H. depressa for each treatment.*

Treatment	A	B	C	D	E
<i>A. lessonii</i>					
n	40	43	17	36	43
Ba/Ca (µmol/mol)	15.8	19.6	18.8	22.9	29.9
SD	3.3	3.6	3.0	4.5	5.5



Mg/Ca (mmol/mol)	37.9	49.2	70.1	89.6	80.4
SD	10	13	19	33	29
<i>H. depressa</i>					
n	26	27	23	25	32
Ba/Ca (μmol/mol)	41.1	41.5	46.0	50.8	74.9
SD	6.2	4.3	3.9	5.7	3.9
Mg/Ca (mmol/mol)	150	135	123	168	177
SD	12	11	6	29	7

704

705 *Table 3. Parameters of the regression analysis and ANOVA tests for significance of the*
 706 *regression. Both average Ba/Ca_{cc} of each experimental condition (n=5) and all chamber-*
 707 *specific Ba/Ca_{cc} (n=133/ 179) were tested versus the Ba/Ca of the 5 treatments.*

			Regression analysis	ANOVA	
Parameter	Species	n	R ²	F-value	p-value
Ba/Ca _{sw} vs Ba/Ca _{cc}	<i>H. depressa</i>	133	0.88	940	<0.01
	<i>A. lessonii</i>	179	0.56	227	<0.01
Ba/Ca _{sw} vs average Ba/Ca _{cc}	<i>H. depressa</i>	5	0.99	247	<0.01
	<i>A. lessonii</i>	5	0.91	32	0.011

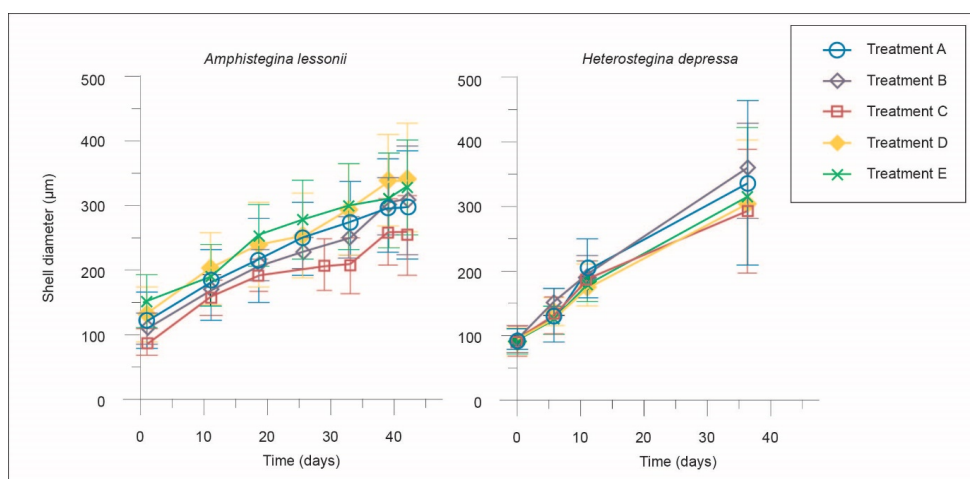
708

709 *Table 4. ANOVA parameters of single-chamber measurements*

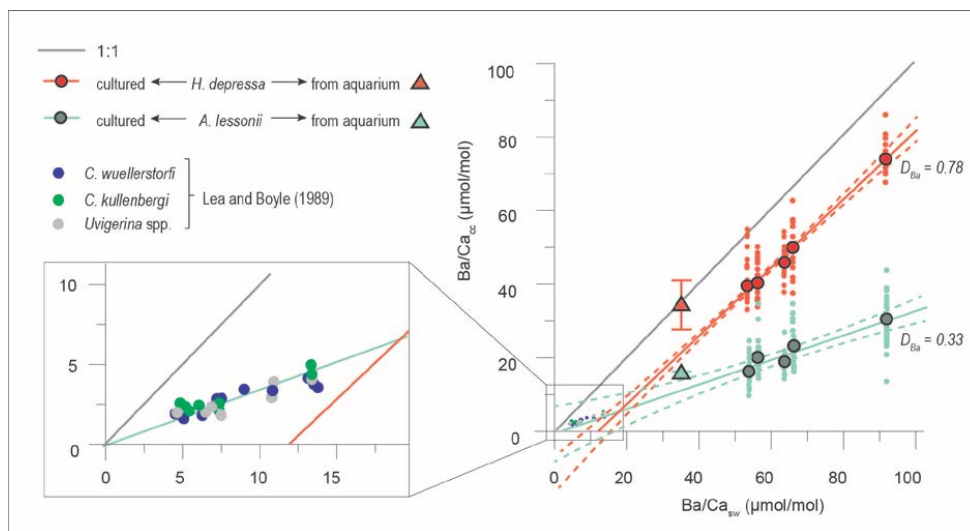
ANOVA	Species	F	p
	<i>A. lessonii</i>	2.47	0.06
	<i>A. lessonii</i> (f-1 and f-2)	0.11	0.744
	<i>H. depressa</i>	6.09	< 0.01



710 **Figures**



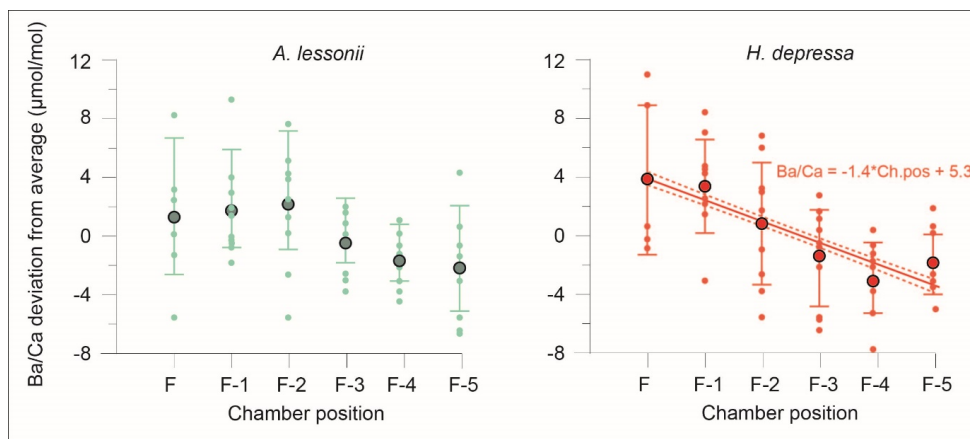
711



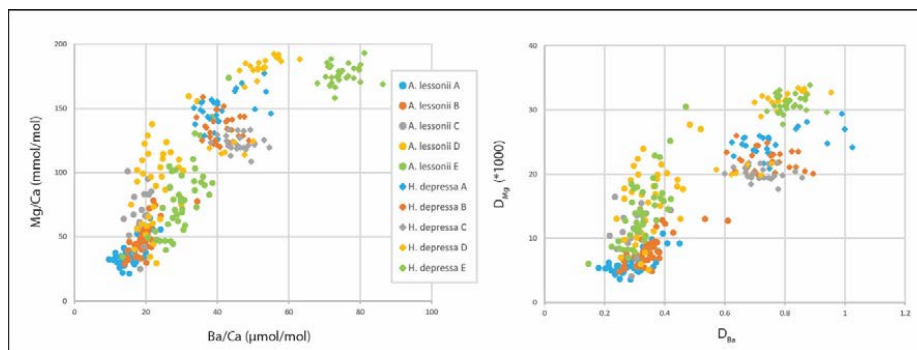
712



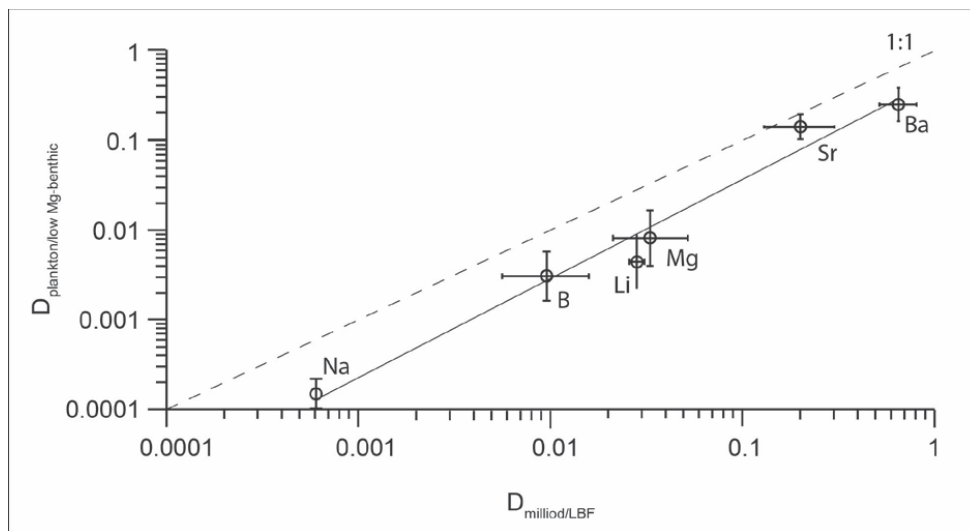
713



714



715





716 **Figure Captions**

717 *Figure 1. Average increase in shell diameter for A. lessonii (left panel) and H. depressa (right*
718 *panel). Dots represent the average of all analysed individuals from one treatment. Error bars*
719 *represent the standard deviation of the mean.*

720

721 *Figure 2. Foraminiferal Ba/Ca as a function of seawater Ba/Ca. Light circles indicate*
722 *individual laser ablation measurements, larger, darker shaded circles represent the average*
723 *Ba/Ca_{cc} for one treatment. Relative standard deviation varies between 16 and 20% for Ba/Ca_{cc}*
724 *in A. lessonii and between 5 and 15% for H. depressa. Average Ba/Ca for the two species*
725 *collected from the aquarium are indicated by triangles (+/- 1 SD) and were not taken into*
726 *account when calculating the regression. Calculated regressions are accompanied by their*
727 *95% confidence intervals (dashed lines) over the Ba/Ca_{sw} range from 50 to 90 µmol/mol. Data*
728 *from Lea and Boyle (1989) is plotted additionally for comparison.*

729

730 *Figure 3. Average (large, darker shaded circles) and single chamber measurements (lighter*
731 *circles) Ba/Ca_{cc}, expressed as their deviation from the mean shell Ba/Ca_{cc} for A. lessonii (left)*
732 *and H. depressa. Error bars represent the standard deviation of the mean, the dashed lines in*
733 *the right panel indicate the 95% confidence intervals for the linear regression.*

734

735 *Figure 4. Relation between the Ba/Ca and Mg/Ca (left panel) and the partition coefficients for*
736 *Ba and Mg (right panel). Every dot represents one single-chamber measurement. The data for*
737 *A. lessonii are indicated by circles, those for H. depressa are represented by diamonds. Every*
738 *treatment (A-E; Table 1) is indicated by a separate color.*

739



740 *Figure 5: Partition coefficients for Li, B, Na, Mg, Sr and Ba for two groups of foraminifera*
741 *(Large Benthic Foraminifera+Miliolids and the low-Mg species). Data on which the average*
742 *partition coefficients are based, are listed in the online supplement, the ranges indicate the*
743 *maximum range in published partition coefficients. The linear regression between the partition*
744 *coefficients for these two groups is described by: $D_{\text{plankton/low Mg-benthic}}=0.3992*D_{\text{miliolid/LBF}} +$*
745 *0.0081. Elemental results for Miliolid species are confined to Mg/Ca and Sr/Ca. Li/Ca ratios*
746 *were taken from Delaney et al. (1985), Hall and Chan (2004a), Marriott et al. (2004), Yu et al.*
747 *(2005), Ni et al. (2007), Bryan and Marchitto (2008), Hathorne et al. (2009), Dawber and*
748 *Tripati (2012) and Evans et al. (2015); B/Ca ratios are from Yu et al. (2005), Yu and Elderfield*
749 *(2007), Foster (2008), Hendry et al. (2009), Allen et al. (2011; 2012), Dawber and Tripati*
750 *(2012), Babila et al. (2014) and Kaczmarek et al. (2015); Na/Ca are from Delaney et al. (1985),*
751 *Ni et al. (2007), Bian et al. (2009), Wit et al. (2013) and Evans et al. (2015); Mg/Ca are from*
752 *Toyofuku et al. (2000), Raja et al. (2005), Yu et al. (2005), Elderfield et al. (2006), Segev and*
753 *Erez (2006), Hendry et al. (2009), Dueñas-Bohórquez et al. (2009; 2011), Dawber and Tripati*
754 *(2012), Wit et al. (2012; 2013), Babila et al. (2014), De Nooijer et al. (2014a), Sadekov et al.*
755 *(2014) and Evans et al. (2015). Foraminiferal Sr/Ca are taken from Raja et al. (2005), Yu et*
756 *al. (2005), Hendry et al. (2009), Dueñas-Bohórquez et al. (2009; 2011), Dawber and Tripati*
757 *(2012), Wit et al. (2013), De Nooijer et al. (2014a) and Evans et al. (2015). Ba/Ca are from*
758 *this study, Lea and Boyle (1989), Lea and Boyle (1991), Lea and Spero (1994), Hall and Chan*
759 *(2004b), Ni et al. (2007), Hönisch et al. (2011) and Evans et al. (2015).*

760